BCSJ

Selected Paper

Design of Coordination Interaction of Zn(II) Complex with Oligo-Aspartate Peptide to Afford a High-Affinity Tag–Probe Pair

Hirokazu Fuchida,[1] Shigekazu Tabata,[1] Naoya Shindo,[1] Ippei Takashima,[1] Qiao Leng,[1] Yuji Hatsuyama,[1] Itaru Hamachi,[2] and Akio Ojida*[1]

[1]Graduate School of Pharmaceutical Sciences, Kyushu University, 3-1-1 Maidashi, Higashi-ku, Fukuoka 812-8582

[2]Department of Synthetic Chemistry and Biological Chemistry, Graduate School of Engineering, Kyoto University, Katsura, Nishikyo-ku, Kyoto 615-8510

E-mail: ojida@phar.kyushu-u.ac.jp
Received: January 27, 2015; Accepted: February 25, 2015; Web Released: March 4, 2015

A complementary recognition pair consisting of a genetically encodable peptide tag and a small molecular probe is a powerful tool to specifically label and manipulate a protein of interest under biological conditions. In this study, we report the redesign of a tag–probe pair comprising an oligo-aspartate peptide tag (such as DDDD) and a binuclear zinc complex. Isothermal-titration calorimetry screening of binding between the series of peptides and zinc complexes revealed that the binding affinity was largely influenced by subtle changes of the ligand structure of the probe. However, the binding was tolerant to differences of the tag peptide sequence. Of those tested, a pair containing a peptide tag (DDAADD) and a binuclear zinc complex possessing 4-chloropyridines (**3**-2Zn(II)) showed the strongest binding affinity ($K_a = 3.88 \times 10^5\,M^{-1}$), which was about 10-fold larger than the conventional pair of D4-peptide tag (DDDD) and **1**-2Zn(II) containing nonsubstituted pyridines ($K_a = 3.73 \times 10^4\,M^{-1}$). The strong binding of this new complementary recognition pair enabled the rapid covalent labeling of a tag-fused maltose binding protein with a fluorescent zinc complex, demonstrating its potential utility in protein analysis.

A complementary recognition pair of a short epitope peptide and a small molecular probe is a versatile analytical tool for a wide variety of protein research. To date, several peptide tag–probe pairs, such as oligo-histidine tag (His-tag) with Ni(II)-NTA (nitrilotriacetic acid)[1] and tetracysteine motif (-Cys-Cys-X-X-Cys-Cys-) with bisarsenical ligand (FlAsH),[2] have been reported. These pairs are widely used for protein purification using affinity column chromatography, protein/peptide immobilization on a microtiter plate, and bioimaging of proteins of interest (POI) under live cell conditions. In contrast to protein labeling techniques using fluorescent proteins (FPs)[3] and enzyme reactions such as SNAP-tag (a protein tag based on human O^6-alkylguanine-DNA alkyltransferase),[4] the use of a genetically encodable peptide tag/small molecular probe pair is a flexible approach for a wide variety of POIs. The pair shows little or no interference with the function of the protein, because its size (1–3 kDa) is smaller than FP (27 kDa) or SNAP-tag (20 kDa). However, the availability of such a useful complementary tag–probe pair is limited, mainly because of the difficulty of rationally designing a recognition pair, where the careful optimization of a probe structure and peptide tag sequence is required to achieve a desirable strong affinity and selective interaction.

We recently developed a binuclear Dpa (2,2′-dipicolylamine)-Zn(II) complex possessing an L-tyrosine scaffold (DpaTyr-Zn(II)) (Figure 1) as a selective binding probe for an oligo-aspartate peptide tag.[5] Based on the coordination interaction between the zinc complex and the aspartate residues of the peptide, the DpaTyr-Zn(II) probe showed a strong binding affinity ($K_a = 6.9 \times 10^5\,M^{-1}$) to D4-tag (Asp-Asp-Asp-Asp) in neutral aqueous conditions (50 mM HEPES, pH 7.2). However, this binding affinity decreased to $4.9 \times 10^4\,M^{-1}$ under high salt concentrations (50 mM HEPES, 100 mM NaCl, pH 7.2) that are relevant to biological environments.[6] Despite this weak binding, there has been little effort to improve the binding affinity by optimizing the probe structure and the peptide tag sequence. In this study, we report the redesign of the coordination interaction between the zinc complex and oligo-aspartate peptide. We found that modification of the ligand structure of the zinc complex largely influenced the binding affinity with tetra-aspartate aspartate peptides. Among the evaluated tag–probe pairs, **3**-2Zn(II) containing 4-chloropyridines displayed the strongest binding affinity toward a peptide with a DDAADD sequence ($K_a = 3.88 \times 10^5\,M^{-1}$). This strong binding pair was successfully used in the rapid covalent labeling of a tag-fused maltose binding protein (MBP) protein with a fluorescent zinc complex.

Results and Discussion

Design of the Binuclear Zn(II) Complex. We initially synthesized a series of binuclear Zn(II) complexes based on a *p*-cresol scaffold, each of which possessed four different

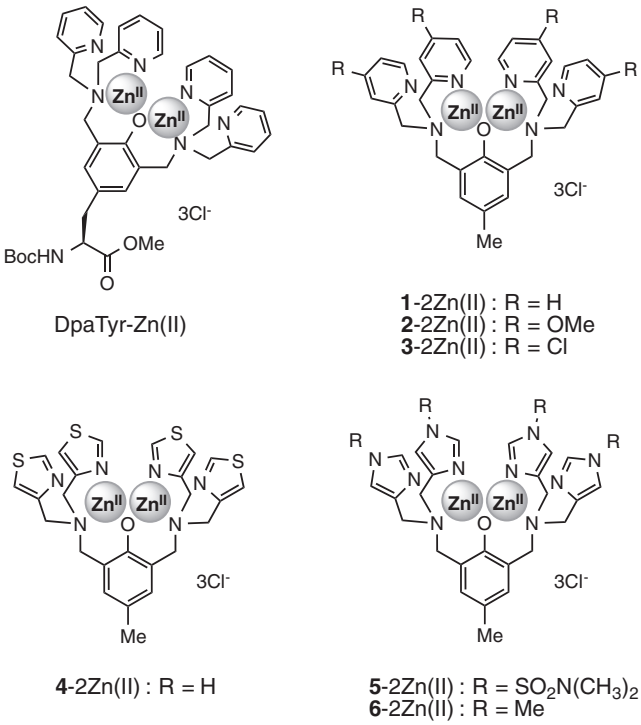

Figure 1. Molecular structures of the binuclear zinc complexes.

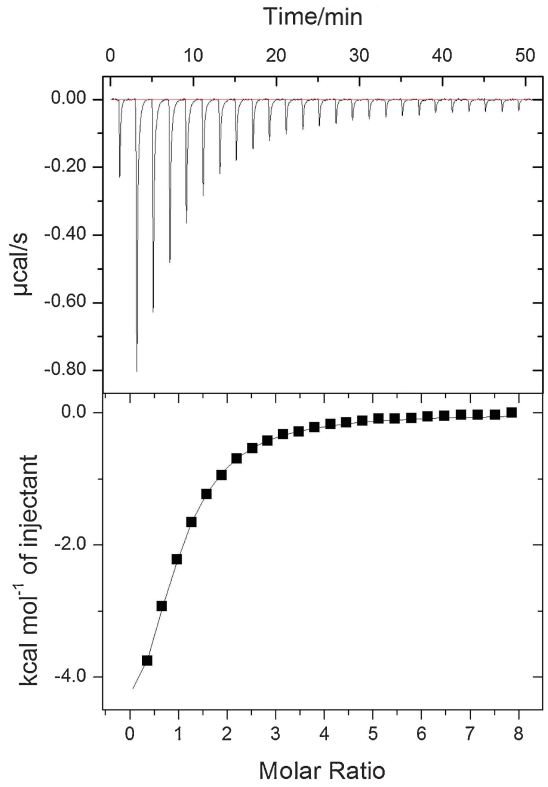

Figure 2. ITC titration curve (upper) and processed data (lower) of **1**-2Zn(II) with DDAADD peptide (Ac-YADDAADD-NH_2). [**1**-2Zn(II)] = 50 µM, [DDAADD] = 2 mM (1.5 µL × 25 injections), 50 mM HEPES, 100 mM NaCl, pH 7.2, 25 °C.

heteroaromatic rings as the zinc coordination units. To evaluate the substitution effect of the pyridine rings, we prepared three Dpa (2,2-dipicolylamine)-type zinc complexes **1**-2Zn(II), **2**-2Zn(II), and **3**-2Zn(II), each of which contained nonsubstituted, 4-chloro-, and 4-methoxypyridine rings, respectively. It was expected that a binuclear zinc complex comprising five-membered heteroaromatic rings could also function as a binding probe for the oligo-aspartate tag. Thus, we prepared a thiazole-type complex **4**-2Zn(II) possessing 4-thiazoles as zinc coordination units. We also prepared imidazole derivatives **5**-2Zn(II) and **6**-2Zn(II), which contained 1-methylimidazoles and 1-(*N*,*N*-dimethylsulfamoyl)imidazoles as the coordination units, respectively. The syntheses and characterization of these zinc complexes are described in Supporting Information (Schemes S1–S6).

Isothermal-Titration Calorimetry Screening of the Peptide Tag–Probe Pair. To screen the binding of the tag–probe pair, we initially evaluated the binding affinities of the binuclear Zn(II) complex **1**-2Zn(II) with a series of oligo-aspartate peptide tags (DDDD, DDADD, DDAADD, and DAAAD) by isothermal-titration calorimetry (ITC). Figure 2 shows a typical ITC titration curve between DDAADD and **1**-2Zn(II), and Table 1 summarizes the results of the ITC experiments. The binding affinity of the conventional pair between **1**-2Zn(II) possessing nonsubstituted pyridines and DDDD (D4-tag) was $3.73 \times 10^4\,M^{-1}$, which was comparable to that of the original DpaTyr-Zn(II)/D4-tag pair. Interestingly, **1**-2Zn(II) could bind to the alanine-inserted tetra-aspartate tags (DDADD and DDAADD) with moderate binding affinities ($K_a = 3.18 \times 10^4$ and $4.23 \times 10^4\,M^{-1}$, respectively), which were comparable to that of DDDD. Furthermore, **1**-2Zn(II) displayed weak binding to the di-aspartate peptide DAAAD ($K_a = 3.18 \times 10^3\,M^{-1}$), which contains two aspartate residues at the i, $i+4$ position. The binding process of **1**-2Zn(II) with the peptides was exothermic enthalpy driven ($\Delta H < 0$) in all cases, but its binding with D4 and DDADD was also driven by the positive entropy change ($\Delta S > 0$). This result implies that the bindings of the latter two cases involve the release of hydration waters, which favors the increased binding affinities of **1**-2Zn(II) with the peptides.[7]

The binding affinities of the other binuclear zinc complexes containing oligo-aspartate peptides were further evaluated by ITC (Table 1). The binding affinities of **2**-2Zn(II) possessing 4-methoxypyridines were comparable to those of **1**-2Zn(II) for all cases tested. However, **3**-2Zn(II) possessing 4-chloropyridines exhibited a stronger binding affinity than **1**-2Zn(II). In particular, the binding affinity with DDAADD was $3.88 \times 10^5\,M^{-1}$, about 10-fold larger than the conventional binding pair of **1**-2Zn(II) and D4 ($K_a = 3.73 \times 10^4\,M^{-1}$). The thermodynamic data suggest that the large negative enthalpy change ($\Delta H = -7.0\,kcal\,mol^{-1}$) of the **3**-2Zn(II)/DDAADD pair contributes to their stronger binding affinity compared with the **1**-2Zn(II)/D4 pair ($\Delta H = -3.35\,kcal\,mol^{-1}$). A comparison of the thermodynamic data of the bindings of the different probes with DDAADD, **2**-2Zn(II) ($\Delta H = -6.54\,kca\,mol^{-1}$, $T\Delta S = -0.38\,kcal\,mol^{-1}$) showed similarities with **1**-2Zn(II) ($\Delta H = -6.53\,kcal\,mol^{-1}$, $T\Delta S = -0.22\,kcal\,mol^{-1}$), while the binding of **3**-2Zn(II) involved a favorable positive entropy change ($T\Delta S = 0.66\,kcal\,mol^{-1}$) as well as a slightly larger negative

Table 1. Summary of ITC Screening to Evaluate the Binding between Zinc Complexes and Oligo-Aspartate Peptides[a),b)]

		DDDD[c)] (D4-tag)	DDADD[d)]	DDAADD[e)]	DAAAD[f)]
1-2Zn(II)	K_a	$(3.73 \pm 0.04) \times 10^4$	$(3.18 \pm 0.31) \times 10^4$	$(4.23 \pm 0.19) \times 10^4$	$(3.18 \pm 0.10) \times 10^3$
	ΔH	-3.35 ± 0.21	-2.56 ± 0.21	-6.53 ± 0.21	-5.47 ± 0.15
	$T\Delta S$	2.69	3.58	-0.22	-0.69
	n	0.82 ± 0.04	0.95 ± 0.06	0.87 ± 0.02	1.03 ± 0.02
2-2Zn(II)	K_a	$(2.98 \pm 0.44) \times 10^4$	$(2.59 \pm 0.31) \times 10^4$	$(3.26 \pm 0.22) \times 10^4$	$(3.28 \pm 0.16) \times 10^3$
	ΔH	-2.46 ± 0.34	-3.50 ± 0.50	-6.54 ± 0.48	-2.10 ± 0.11
	$T\Delta S$	3.64	2.52	-0.38	2.70
	n	0.85 ± 0.10	0.75 ± 0.09	0.72 ± 0.04	0.98 ± 0.04
3-2Zn(II)	K_a	$(2.08 \pm 0.22) \times 10^5$	$(1.23 \pm 0.13) \times 10^5$	$(3.88 \pm 0.37) \times 10^5$	$(2.99 \pm 0.19) \times 10^3$
	ΔH	-1.34 ± 0.04	-1.56 ± 0.07	-7.00 ± 0.12	-3.80 ± 0.13
	$T\Delta S$	5.90	5.39	0.66	2.31
	n	0.76 ± 0.02	0.64 ± 0.02	0.78 ± 0.01	0.86 ± 0.02
4-2Zn(II)	K_a	$(5.44 \pm 0.31) \times 10^4$	$(3.64 \pm 0.17) \times 10^4$	$(7.56 \pm 0.23) \times 10^4$	$(8.12 \pm 0.11) \times 10^3$
	ΔH	-2.67 ± 0.05	-3.84 ± 0.08	-8.43 ± 0.07	-6.49 ± 0.04
	$T\Delta S$	3.78	2.38	-1.77	-1.15
	n	0.88 ± 0.01	0.87 ± 0.02	0.92 ± 0.01	0.96 ± 0.00
5-2Zn(II)	K_a	$(2.71 \pm 0.56) \times 10^4$	$(2.06 \pm 0.32) \times 10^4$	$(2.36 \pm 0.21) \times 10^4$	$(1.76 \pm 0.11) \times 10^3$
	ΔH	-1.04 ± 0.17	-1.37 ± 0.21	-4.25 ± 0.5	-4.33 ± 0.44
	$T\Delta S$	5.01	4.50	1.72	0.10
	n	0.93 ± 0.13	0.93 ± 0.12	0.85 ± 0.08	0.90 ± 0.08
6-2Zn(II)	K_a	$<10^3$	$<10^3$	$<10^3$	—[g)]
	ΔH				
	$T\Delta S$				
	n				

a) n: stoichiometry, K_a: binding constant (M^{-1}), ΔH: enthalpy (kcal mol^{-1}), $T\Delta S$: entropy (kcal mol^{-1}). b) Measurement conditions: 50 mM HEPES, 100 mM NaCl, pH 7.2, 25 °C. c) D4 peptide: Boc-$(Asp)_4$-NH_2. d) DDADD peptide: Ac-YADDADD-NH_2. e) DDAADD peptide: Ac-YADDAADD-NH_2. f) DAAAD peptide: Ac-DAAAD-NH_2. g) Not measured.

enthalpy change ($\Delta H = -7.00$ kcal mol^{-1}) compared with **1**-2Zn(II), both of which contribute to the strong binding affinity of **3**-2Zn(II) with DDAADD. Thus, a subtle structural change of the probe markedly influenced the binding affinity of the tag–probe pair by perturbation of the binding thermodynamics. This suggests that a delicate structural design is required to achieve a tighter binding with the probe that operates under aqueous conditions.[8]

In the series of zinc complexes possessing the five-membered heteroaromatic rings, the thiazole-type complex **4**-2Zn(II) showed a slightly higher binding affinity than **1**-2Zn(II). The binding affinities of **5**-2Zn(II) possessing 1-(*N*,*N*-dimethylsulfamoyl)imidazoles were slightly weaker than **1**-2Zn(II). The binding processes of these zinc complexes are exothermic enthalpy driven ($\Delta H < 0$) in all cases, as also observed for the pyridine-type probes. Interestingly, **6**-2Zn(II) possessing *N*-methylimidazoles showed a very weak binding affinity with all of the tetra-aspartate peptides ($K_a < 10^3$ M^{-1}). The weak binding of **6**-2Zn(II) cannot be explained by the ITC result because of the lack of thermodynamic data. However, we speculated that the weak binding of **6**-2Zn(II) might be attributable to the stronger basicity of the *N*-methylimidazole rings compared with **5**-2Zn(II), which contains the more electron-deficient 1-(*N*,*N*-dimethylsulfamoyl)imidazoles. The calculated pK_a value of the conjugated acid of 1-methylimidazole is 7.01, which is significantly larger than that of 1-(*N*,*N*-dimethylsulfamoyl)imidazole (p$K_a = 2.41$).[9] Thus, the strong basicity of 1-methylimidazole might reduce the Lewis acidity of the coordinated zinc ions of **6**-2Zn(II), resulting in its weak binding with the tetra-aspartate peptide.

Fluorescence Evaluation of the Binding of the Peptide Tag–Probe Pair. Binding of the zinc complexes with the oligo-aspartate peptide was evaluated by fluorescence titration to confirm the results of the ITC screening. For fluorescence titration, we prepared a fluorescent DDAADD peptide (hc-KDDAADD) labeled with 7-hydroxycoumarin at the ε-amino group of the lysine reside (Figure 3a). When **3**-2Zn(II) was added to the aqueous solution of hc-KDDAADD (5 μM in 50 mM HEPES, 100 mM NaCl, pH 7.2), the fluorescence of the 7-hydroxycoumarine decreased to approximately 20% of its original intensity (Figure 3b). This fluorescence change might be due to the heavy metal ion effect of zinc ions and/or the micro-pH change induced by the probe binding. The change of fluorescence intensity at 446 nm evaluated by curve fitting analysis was 5.1×10^5 M^{-1}, which is comparable to that observed in the ITC experiment ($K_a = 3.88 \times 10^5$ M^{-1}) (Figure 3c). The binding stoichiometry between **3**-2Zn(II) and hc-DDAADD was evaluated by fluorescence Job's plot, which clearly indicates that their binding stoichiometry is 1:1 (Figure S1). Fluorescence titration was performed with the other zinc complexes and the results are summarized in Table 2. The binding affinity of **1**-2Zn(II) was 5.87×10^4 M^{-1}, approximately 10-fold lower than that of **3**-Zn(II), confirming the affinity-enhancing effect of the chloride groups on its pyridine rings. The binding affinity of the thiazole-type complex **4**-2Zn(II) was 1.18×10^5 M^{-1}, a slightly higher value than that of **1**-2Zn(II). Regarding the imidazole-

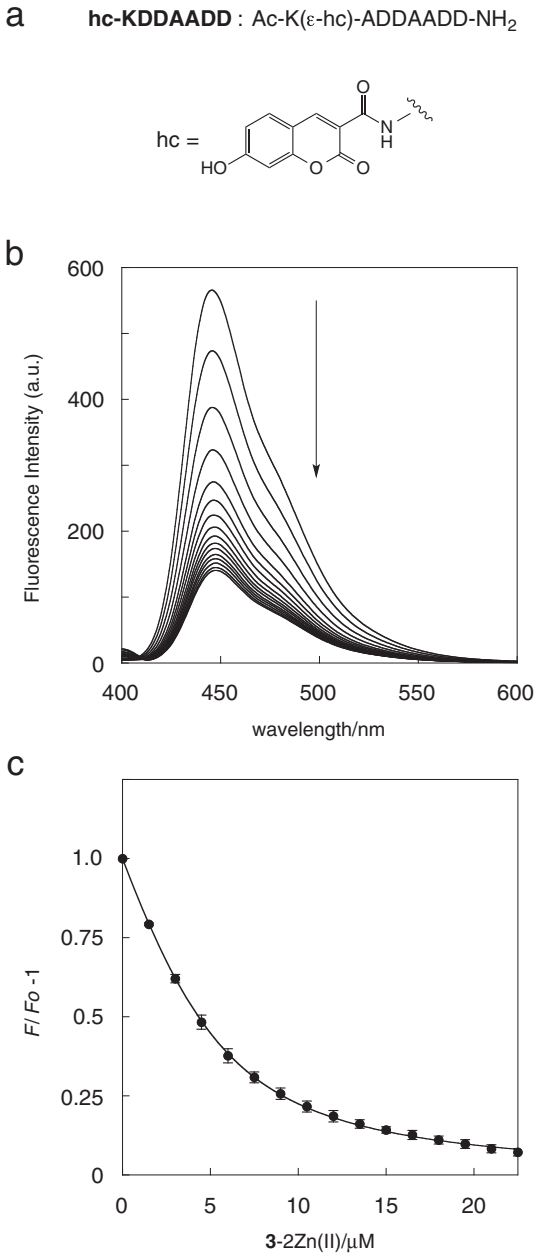

Figure 3. Fluorescence titration of the 7-hydroxycoumarin-appended oligo-aspartate peptide (hc-KDDAADD) with zinc complexes. (a) Structure of the hc-KDDAADD peptide. (b) Fluorescence spectral change of the hc-KDDAADD peptide (5 μM) upon addition of **3**-2Zn(II) (0–20 μM). (c) Curve-fitting analysis of the fluorescence emission change at 446 nm. The error bars represent standard deviations obtained by the triplicate experiments. Measurement conditions: 50 mM HEPES, 100 mM NaCl, pH 7.2, 25 °C, $\lambda_{ex} = 400$ nm.

type complexes, **5**-2Zn(II) showed a slightly weaker binding affinity ($K_a = 2.76 \times 10^5\,M^{-1}$) than **1**-2Zn(II), whereas the binding affinity of **6**-2Zn(II) was very weak ($K_a < 10^3\,M^{-1}$) under the aqueous conditions. The order of the binding affinities of the zinc complexes shown in Table 2 is the same as that obtained by the ITC experiments (Table 1), suggesting the validity of the present binding data obtained by the two distinct methods.

CD Conformation Analysis of Peptide Binding with the Probe. It is reasonable to assume that the zinc complexes induced a folded peptide structure in the binding complex, especially in the case of longer peptides such as DDAADD and DAAAD, both of which contain aspartate residues that are involved in binding at the distal positions. To clarify this, we initially performed circular dichroism (CD) measurements of the DAAAD peptide possessing the two aspartate residues at the i, $i + 4$ position (Figure 4). DAAAD showed a negative Cotton peak around 200 nm in the absence of **3**-2Zn(II), indicative of the nonfolded random structure in its free form. In the binding complex of DAAAD with **3**-2Zn(II), the negative Cotton peak around 200 nm disappeared and the strong induced CD (*i*-CD) peaks appeared in the wide wavelength region from 350 to 190 nm. The large *i*-CD observed at over 300 nm ($\theta_{max} = 310$ nm), which corresponds to the absorption region of the zinc-phenolate moiety, suggested that a chiral environment was introduced at the coordination sphere of **3**-2Zn(II) upon binding to the peptide. However, these Cotton peaks did not involve the representative CD patterns of the folded peptide such as α-helix and β-turn. Almost the same trend was observed in the CD measurement of the binding complexes of **3**-2Zn(II) with tetra-aspartate peptides such as DDDD, DDADD, and DDAADD (Figure S2). These peptides lost their nonfolded random structures and showed unique *i*-CD patterns distinct from each other in the binding complexes with **3**-2Zn(II). Although these CD patterns might reflect the folded peptide structures, they did not involve the typical Cotton peaks of α-helix or β-turn. Thus, the CD analysis was unable to suggest the conformation of the folded peptides binding with the zinc complex.

Covalent Labeling of the Tag-Fused Protein with the Zinc Complex. The utility of the strong binding affinity of DDAADD-tag/**3**-2Zn(II) probe pair ($K_a = 3.88 \times 10^5\,M^{-1}$ determined by ITC experiment) was assessed by the binding-induced covalent labeling of the tag-fused protein.[10] For this purpose, we prepared MBP tethered to a cysteine-containing CA6DDAADD-tag (CAAAAAADDAADD) and a fluorescent Dpa-Zn(II) complex possessing a reactive chloroacetyl group.[11] It was expected that their complementary strong binding would enhance the nucleophilic reaction between the reactive tag and the probe to produce the covalently labeled MBP (Figure 5a). The synthesis of the reactive zinc complex **7**-2Zn(II), which possesses a fluorescent coumarin unit, is described in Scheme 1. Compound **9** was conjugated with Boc-Lys-OH to give **10**, which was deprotected by TFA and then conjugated with α-chloroacetyl *O*-succinimidyl ester to yield the reactive fluorescent unit **11**. The ligand unit was synthesized from the bis(*o*-chloromethyl)cresol **12**[12] and the dipicolylamine **13** to give **14**, which was deprotected by treatment with hydrazine to yield **15**. Finally, both units were conjugated and the product was purified by HPLC to give the pure ligand **7**. When **7**-2Zn(II) (5 μM) (Figure 5c), which was prepared by the treatment of **7** with 2 equiv of $ZnCl_2$, was added to an aqueous solution of the CA6DDAADD-tag-fused MBP (1 μM in 50 mM HEPES, 100 mM NaCl, pH 7.2), rapid labeling occurred. In-gel fluorescence analysis showed that the fluorescent band corresponding to MBP labeled with **7**-2Zn(II) gradually increased within 30 min (Figures 5b and 5d). MALDI-TOF mass analysis identified a new peak corresponding to the covalent adduct of the tag-

Table 2. Summary of the Binding Constants (K_a, M^{-1}) of the Zinc Complexes with the hc-KDDAADD Peptide as Determined by Fluorescence Titration[a),b)]

	1-2Zn(II)	**2**-2Zn(II)	**3**-2Zn(II)	**4**-2Zn(II)	**5**-2Zn(II)	**6**-2Zn(II)
K_a/M^{-1}	5.87×10^4	6.25×10^4	5.14×10^5	1.18×10^5	2.76×10^4	$<10^3$
	(4.23×10^4)	(3.26×10^4)	(3.88×10^5)	(7.56×10^4)	(2.36×10^4)	($<10^3$)

a) Measurement conditions: 50 mM HEPES, 100 mM NaCl, pH 7.2, 25 °C. b) The binding constants in parentheses are the values determined in the ITC experiment (Table 1).

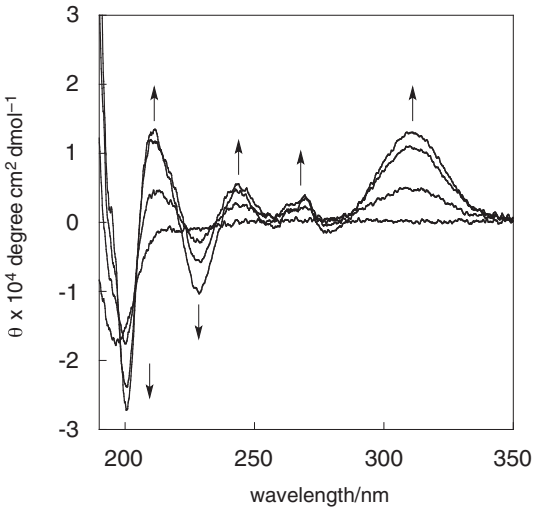

Figure 4. CD titration of DAAAD peptide (50 μM) with **3**-2Zn(II) (0, 25, 50, and 100 μM). Measurement conditions: H_2O, pH 7.4, 25 °C.

fused MBP with **7**-2Zn(II) (Figure S3). However, none of the fluorescent bands were detected by in-gel fluorescence analysis when the labeling reaction was conducted in the presence of a high concentration of inorganic pyrophosphate (PPi, 2.5 mM), a strong binder of the binuclear zinc complex (Figure S2).[5c,12] This result suggests that the selective binding between the tag and the probe is critical to the covalent labeling of the tag-fused MBP. Binding-induced MBP labeling was also conducted using the conventional D4-tag/Dpa-Zn(II) probe pair (Figure 5b). In-gel fluorescence analysis revealed that the labeling of CA6D4 (CAAAAAADDDD)-tag-fused MBP with **8**-2Zn(II) was slower than that of the new tag–probe pair; the initial reaction rate (ΔF, min^{-1}) of MBP labeling using the CA6D4-tag/**8**-2Zn(II) probe pair was 0.59, which was 2.7-fold smaller than that using CA6DDAADD-tag/**7**-2Zn(II) probe pair ($\Delta F = 1.61\ min^{-1}$).[13] This result demonstrates an advantage of the new tag–probe pair over the previous one for binding-induced protein labeling, in which the strong binding affinity of the new pair facilitates the rapid and efficient labeling of the tag-fused protein under low concentration conditions.

Conclusion

We developed a new tag–probe pair consisting of a DDAADD-tag and **3**-2Zn(II) probe, which shows approximately 10-fold stronger binding affinity than the conventional pair of DDDD and **1**-2Zn(II). We now plan further application of this tag–probe pair for fluorescence imaging in living cells and affinity purification of a tag-fused protein. We also envision that further optimization of the probe structure and peptide sequence will provide a tag–probe pair with a better binding affinity. The present data reveal that a subtle difference in the probe structure resulted in a large difference in peptide binding affinity. This result suggests there is scope to develop a new tag–probe pair with a strong binding affinity suitable for protein analysis and manipulation under crude biological conditions.

Experimental

Synthesis of the Zinc Complexes. The zinc complexes **1**–**5**-2Zn(II) were prepared by treatment of the ligand **1**–**5** with an aqueous solution of $ZnCl_2$ (2 equiv) in MeOH at rt for 30 min. After removal of the solvent by evaporation, the residue was dissolved in distilled H_2O, and the solution was filtered through cellulose acetate filter and lyophilized. The solid was collected by filtration, washed with AcOEt, and dried in vacuo to give a powder. In the case of **6**-2Zn(II), the ligand **6** was difficult to handle in air due to its hygroscopic property. Thus, the zinc complex was prepared by the treatment of the aqueous solution of **6** with 2 equiv of $ZnCl_2$, in which the concentration of **6** was determined by UV titration ($\lambda_{abs} = 295$ nm) with $ZnCl_2$ in the solution (50:50, v/v) of CH_3CN and 50 mM HEPES, 100 mM NaCl, pH 7.2.

1-2Zn(II) (88%) Anal Calc for $C_{33}H_{34}N_6O{\cdot}2Zn{\cdot}3Cl{\cdot}HCl{\cdot}2H_2O$: C, 47.23; H, 4.56; N, 10.01%. Found: C, 47.26; H, 4.22; N, 10.01%. ESI-MS m/z 751.13 $[C_{33}H_{33}ClN_6OZn_2 + 2OH + Na]^+$.

2-2Zn(II) (94%) Anal Calc for $C_{37}H_{42}N_6O_5{\cdot}2Zn{\cdot}3Cl{\cdot}HCl{\cdot}H_2O$: C, 47.21; H, 4.71; N, 8.93%. Found: C, 47.20; H, 4.48; N, 8.99%. ESI-MS m/z 871.16 $[C_{37}H_{41}ClN_6O_5Zn_2 + 2OH + Na]^+$.

3-2Zn(II) (92%) Anal Calc for $C_{33}H_{30}Cl_4N_6O{\cdot}2Zn{\cdot}3Cl{\cdot}HCl{\cdot}H_2O$: C, 41.33; H, 3.36; N, 8.76%. Found: C, 41.64; H, 3.33; N, 8.34%. ESI-MS m/z 888.96 $[C_{33}H_{29}Cl_5N_6OZn_2 + 2OH + Na]^+$.

4-2Zn(II) (94%) Anal Calc for $C_{25}H_{26}N_6OS_4{\cdot}2Zn{\cdot}3Cl{\cdot}HCl{\cdot}H_2O$: C, 35.52; H, 3.34; N, 9.94%. Found: C, 35.40; H, 3.18; N, 9.90%. ESI-MS m/z 772.94 $[C_{25}H_{25}ClN_6OS_4 + 2OH + Na]^+$.

5-2Zn(II) (86%) Anal Calc for $C_{33}H_{50}N_{14}O_9S_2{\cdot}2Zn{\cdot}3Cl{\cdot}HCl{\cdot}H_2O$: C, 32.87; H, 4.35; N, 16.04%. Found: C, 32.87; H, 4.35; N, 15.92%. ESI-MS m/z 1135.08 $[C_{33}H_{49}N_{14}O_9S_4 + 2OH + Na]^+$.

Synthesis of the Labeling Probe. Synthesis of 10: A solution of Boc-Lys-OH (500 mg, 2.03 mmol), **9** (717 mg, 2.00 mmol), and DIEA (523 μL, 3.00 mmol) in dry DMF (15.0 mL) was stirred at rt for 3.5 h. After removal of the solvent under reduced pressure, the residue was diluted with water and extracted with AcOEt. The extracts were washed with brine, dried over $MgSO_4$, and concentrated by evaporation. The

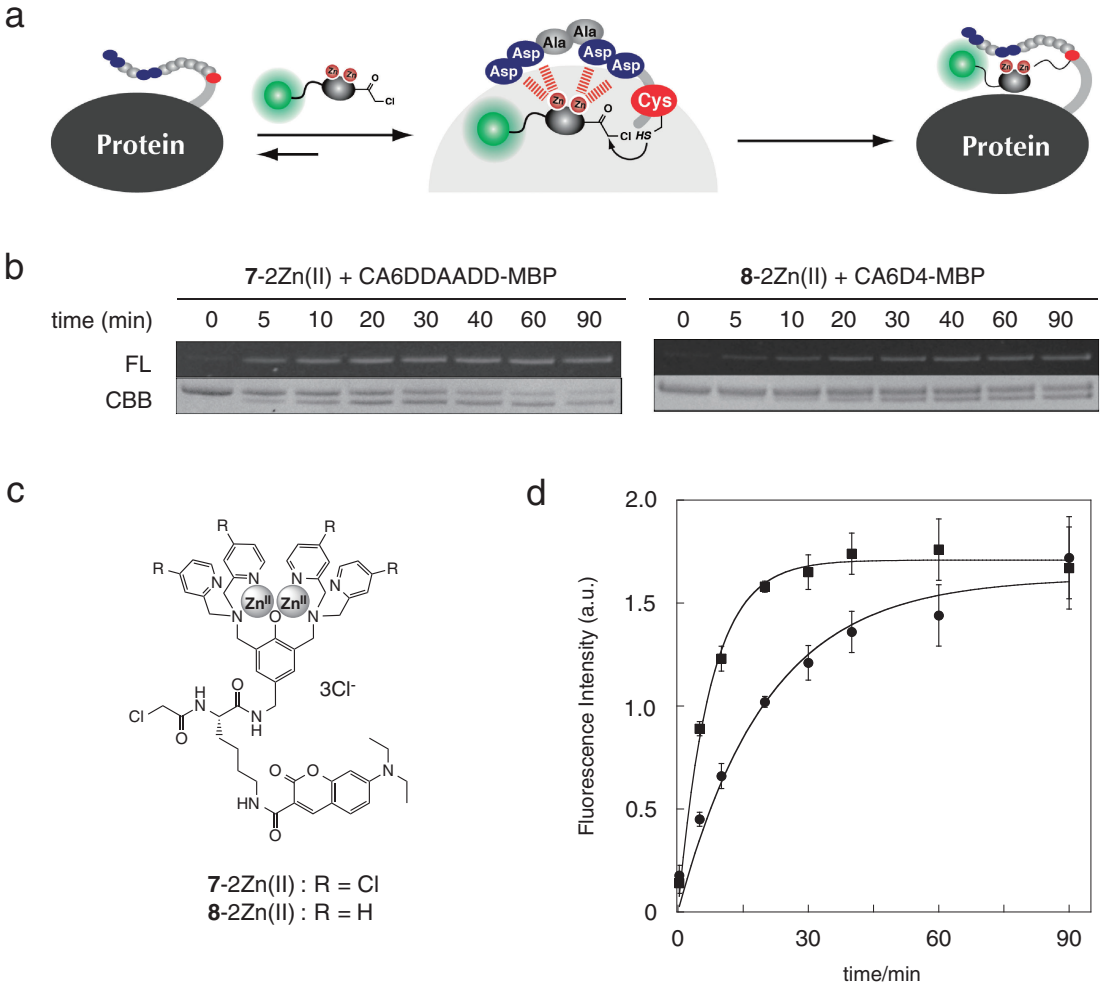

Figure 5. (a) Schematic illustration of the covalent labeling of the CA6DDAADD-tag-fused protein with the reactive binuclear zinc complex. (b) In-gel fluorescence (FL) and CBB analyses of the covalent labeling of CA6DDAADD-tag-fused maltose binding protein (MBP) with **7**-2Zn(II) (left) and CA6D4-tag-fused MBP with **8**-2Zn(II) (right). Labeling conditions: [tag-fused MBP] = 1 μM, [zinc complex] = 5 μM, 50 mM HEPES, 100 mM NaCl, pH 7.2, 18 °C. (c) Structures of the zinc complexes used for the covalent labeling of tag-fused MBP. (e) Time trace plot of the labeling reactions shown in Figure 5b; CA6DDAADD-tag-fused MBP with **7**-2Zn(II) (■), CA6D4-tag-fused MBP with **8**-2Zn(II) (●). The error bars represent standard deviations obtained by the triplicate experiments.

residue was purified by flash column chromatography on SiO_2 ($CHCl_3$:MeOH = 20:1) to give **10** (558 mg, 56%) as a yellow amorphous powder. ^{1}H NMR (400 MHz, $CDCl_3$): δ 8.92–8.89 (1H, t, J = 5.6 Hz), 8.71 (1H, s), 7.42–7.40 (1H, d, J = 9.2 Hz), 6.64–6.61 (1H, dd, J = 2.0 Hz, 9.2 Hz), 6.48–6.47 (1H, d, J = 2.4 Hz), 5.31–5.29 (1H, d, J = 8.0 Hz), 4.27 (1H, brs), 3.46–3.41 (6H, q, J = 7.2 Hz), 1.91–1.79 (2H, m), 1.66–1.62 (2H, m), 1.46 (2H, m), 1.42 (9H, s), 1.24–1.20 (6H, t, J = 7.0 Hz). ESI-MS m/z found 534.22 for $C_{25}H_{35}N_3O_7$ $[M + 2Na]^+$.

Synthesis of 11: To a cooled (0 °C) solution of **10** (200 mg, 0.41 mmol) in dry CH_2Cl_2 (3 mL) was added dropwise TFA (3 mL). The reaction mixture was stirred at rt for 2 h. After removal of the solvent under reduced pressure, the reside was dissolved in toluene and evaporated to give the deprotected product (as mono TFA salt, 207 mg, quant.) as a yellow amorphous powder. ^{1}H NMR (400 MHz, $CDCl_3$): δ 9.14–9.12 (1H, t, J = 2.6 Hz), 8.53 (1H, s), 7.98 (2H, brs), 7.38–7.36 (1H, d, J = 8.8 Hz), 6.64–6.62 (1H, d, J = 9.2 Hz), 6.43 (1H, s), 4.08 (1H, s), 3.42–3.39 (6H, m), 2.02 (2H, brs), 1.59–1.44 (4H, m), 1.21–1.18 (6H, t, J = 7.0 Hz). ESI-MS m/z found 412.19 for $C_{20}H_{27}N_3O_5$ $[M + Na]^+$.

A solution of the deprotected product (100 mg, 0.21 mmol), α-chloroacetyl *N*-hydroxysuccinimidyl ester (50 mg, 0.26 mmol), and DIEA (89 μL, 0.51 mmol) in dry DMF (5 mL) was stirred at rt for 1 h. After removal of the solvent under reduced pressure, the residue was purified by flash column chromatography on SiO_2 to give **11** (88 mg, 91%) as a yellow solid. ^{1}H NMR (400 MHz, $CDCl_3$): δ 8.97 (1H, brs), 8.69 (1H, s), 7.43–7.41 (1H, d, J = 8.8 Hz), 6.64–6.62 (1H, d, J = 6.8 Hz), 6.47 (1H, s), 4.56 (1H, s), 4.04 (2H, s), 3.46–3.41 (6H, m), 1.98–1.86 (2H, m), 1.64 (2H, m), 1.45 (2H, m), 1.24–1.20 (6H, t, J = 7.0 Hz). ESI-MS m/z found 488.16 for $C_{22}H_{28}ClN_3O_6$ $[M + Na]^+$.

Synthesis of 14: A solution of **12** (26 mg, 0.075 mmol),[14] **13** (48 mg, 0.18 mmol), KI (3.0 mg, 0.018 mmol), and K_2CO_3 (32 mg, 0.23 mmol) in dry DMF (2 mL) was stirred at rt over-

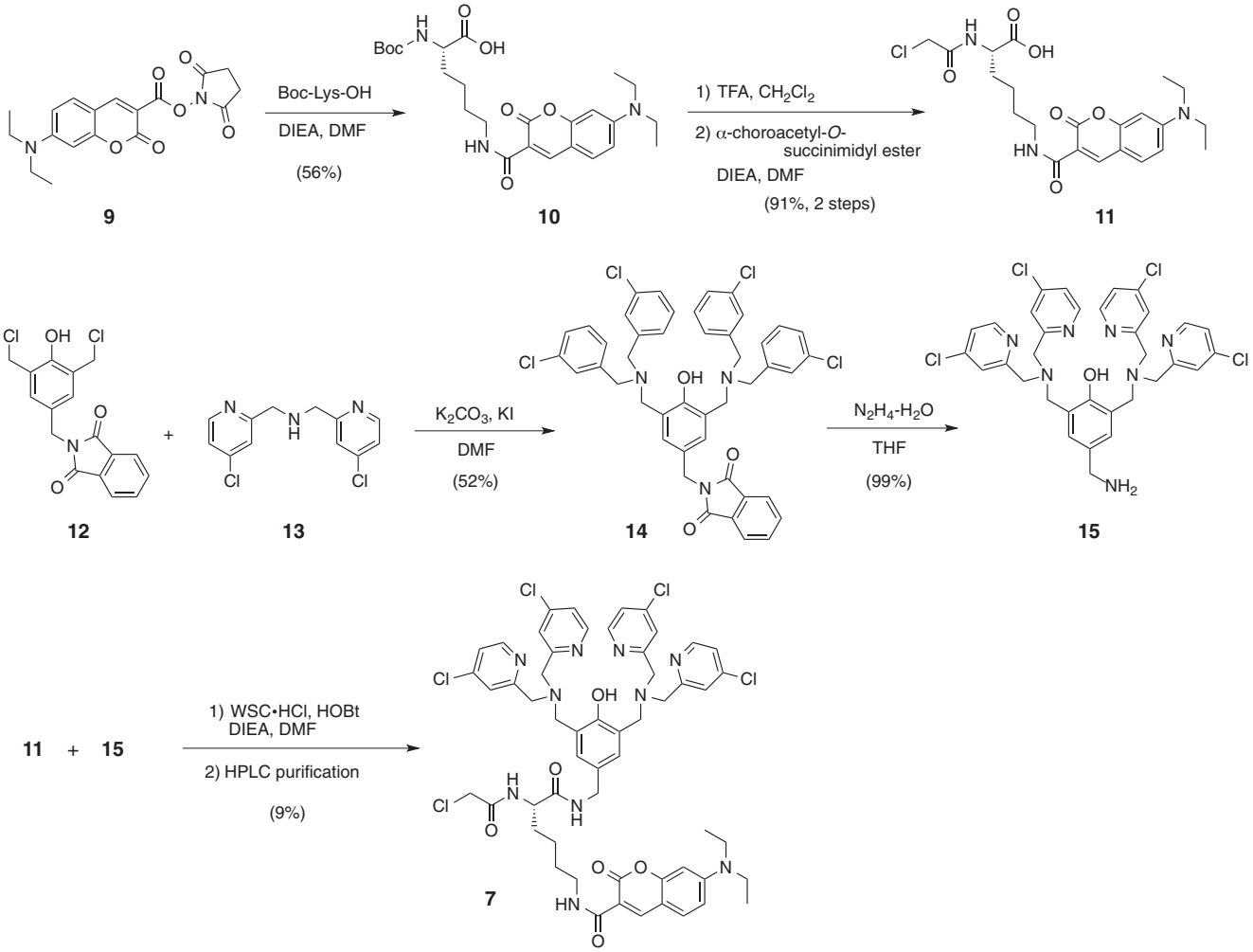

Scheme 1. Synthesis of the labeling probe.

night. After removal of the solvent under reduced pressure, the residue was dissolved in sat. $NaHCO_3$ and extracted with AcOEt. The extracts were dried over $MgSO_4$ and concentrated by evaporation. The residue was purified by flash column chromatography on SiO_2 ($CHCl_3$:MeOH:NH_3 = 500:10:1) to give **14** (32 mg, 52%) as a colorless amorphous powder. ^{1}H NMR (400 MHz, $CDCl_3$): δ 8.39–8.37 (4H, d, J = 5.6 Hz), 7.81–7.79 (2H, m), 7.66–7.78 (2H, m), 7.50 (4H, s), 7.11–7.10 (4H, d, J = 5.2 Hz), 4.71 (2H, s), 3.83 (8H, s), 3.77 (4H, s). ESI-MS m/z found 836.13 for $C_{41}H_{33}Cl_4N_7O_3$ $[M + Na]^+$.

Synthesis of 15: A solution of **14** (32 mg, 0.039 mmol) and hydrazine monohydrate (145 µL) in THF (2.0 mL) was stirred at rt overnight. After removal of the solvent by evaporation, the residue was dissolved in sat. $NaHCO_3$ and extracted with $CHCl_3$. The extracts were dried over $MgSO_4$ and concentrated by evaporation to give **15** (27 mg, 99%) as a yellow oil. ^{1}H NMR (400 MHz, $CDCl_3$): δ 8.42–8.29 (4H, m), 7.50–7.45 (4H, m), 7.13–7.09 (4H, m), 7.05 (2H, s), 3.86 (8H, s), 3.79 (4H, s), 3.73 (2H, s). ESI-MS m/z found 684.14 for $C_{33}H_{31}Cl_4N_7O_6$ $[M + H]^+$.

Synthesis of 7: A solution of **11** (27 mg, 0.057 mmol), **15** (26 mg, 0.038 mmol), WSC•HCl (22 mg, 0.11 mmol), HOBt•H_2O (17 mg, 0.11 mmol), and DIEA (30 µL, 0.17 mmol) in dry DMF (1 mL) was stirred at rt for 3 h. After dilution with sat. $NaHCO_3$, the mixture was extracted with AcOEt. The extracts were dried over $MgSO_4$ and concentrated by evaporation. The residue was purified by HPLC (column; YMC-Actus Triart C18, 20 × 250 mm) using CH_3CN (0.1% TFA)/H_2O (0.1% TFA) solvent system with a linear gradient mode (CH_3CN (0.1% TFA)/H_2O (0.1% TFA) = 50/50 → 80/20 (0 → 50 min)) to give **7** (as tetra TFA salt, 4.9 mg, 9%) as a yellow solid. ^{1}H NMR (400 MHz, $CDCl_3$): δ 8.83 (1H, s), 8.65 (1H, s), 8.48–8.47 (4H, d, J = 4.8 Hz), 7.43 (4H, s), 7.42–7.39 (1H, d, J = 9.2 Hz), 7.25 (4H, s), 7.14 (2H, s), 6.63–6.61 (1H, d, J = 9.2 Hz), 6.47 (1H, s), 4.44 (1H, m), 4.21 (8H, s), 4.07 (4H, s), 4.06 (2H, s), 4.05 (2H, s), 3.46–3.40 (6H, m), 1.94–1.80 (2H, m), 1.64–1.56 (2H, s), 1.44–1.40 (2H, m), 1.24–1.20 (6H, t, J = 7.2 Hz). ESI-TOF-MS m/z found 1131.31 for $C_{57}H_{59}Cl_5N_8O_6$ $[M + H]^+$.

Isothermal Titration Calorimetry (ITC) Measurement. ITC titration was performed with MicroCal Auto-iTC200 (GE Healthcare). All measurements were conducted at 298 K. Typically, a solution of the peptide (2–7 mM) in a buffer solution (50 mM HEPES, 100 mM NaCl, pH 7.2) was injected stepwise (1.5 µL × 25 times) to a solution of the metal complex of DpaTyr (50–300 µM) in the same solvent system. The measured heat flow was recorded as function of time and converted into enthalpies (ΔH) by integration of the appropriate reaction

peaks. Dilution effects were corrected for by subtracting the result of a blank experiment with an injection of the HEPES solution into cell under identical experimental conditions. The binding parameters (K_{app}, ΔH, ΔS, n) were evaluated by applying one site model using the software Origin 7 (Origin Lab).

Fluorescence Titration. Fluorescence spectra were recorded on a Perkin-Elmer LS55 spectrofluorophotometer. The titration experiments were performed at 25 °C using a solution of hc-DDAADD peptide in buffer solution (50 mM HEPES, 100 mM NaCl, pH 7.2) in a quartz cell. The concentration of the hc-DDAADD peptide was determined based on the reported extinction coefficient of 7-hydroxycoumarine-3-carboxamide ($\varepsilon_{370nm} = 12300\,M^{-1}\,cm^{-1}$). The fluorescence emission spectra ($\lambda_{ex} = 400$ nm) were measured after the addition of a freshly prepared aqueous solution of the zinc complexes with a micropipet. Fluorescence titration curves ($\lambda_{em} = 446$ nm) were analyzed using nonlinear least-square curve-fitting to evaluate the binding constant (K_a, M^{-1}).

Circular Dichroism (CD) Measurement. CD spectra were recorded using a JASCO J-720W spectropolarimeter. The aqueous stock solution of the **3**-2Zn(II) was added into the solution of the peptide (50 μM) in water (pH 7.4, adjusted by 10 mM NaOH), and the CD spectrum was measured from 350 to 190 nm (scan speed; 50 nm min^{-1}) at 25 °C using a quartz cell (0.1 cm path length). Each spectrum represents the average of 10 scans with smoothing to reduce noise.

Covalent Labeling of MBP Protein. A solution of the tag-fused MBP (1 μM final concentration) in degassed 50 mM HEPES, 100 mM NaCl, 20 μM TCEP, pH 7.2 was mixed with the zinc complex (**7**-Zn(II) or **8**-2Zn(II), 5 μM in final concentration). The reaction mixture (total volume 100 μL) was incubated at 18 °C for 90 min, in which time the mixture (8 μL) was sampled at the appropriate reaction time and then immediately mixed with 10 mM inorganic pyrophosphate (2 μM) to quench the reaction. After addition of the sampling buffer and heating at 95 °C for 2 min, the samples were subjected to SDS-PAGE. The in-gel fluorescence and CBB analyses were performed with LAS-4000 lumino image analyzer (FUJIFILM) by EPI (365 nm excitation, Y515Di filter) and DIA-W mode, respectively.

We appreciate the technical support from the Research Support Center, Graduate School of Medical Sciences, Kyushu University. This work was performed under the Cooperative Research Program of "Network Joint Research Center for Materials and Devices." A. O. acknowledges Takeda Science Foundation for financial support.

Supporting Information

Experimental data of Job's plot and CD measurement, and the protein labeling reaction. Syntheses of the zinc complexes and the peptides, and expression of the tag-fused MBPs. This material is available electronically on J-STAGE.

References

1 a) S. Uchinomiya, H. Nonaka, S. Wakayama, A. Ojida, I. Hamachi, *Chem. Commun.* **2013**, *49*, 5022. b) M. Taki, F. Asahi, T. Hirayama, Y. Yamamoto, *Bull. Chem. Soc. Jpn.* **2011**, *84*, 386. c) M. Kamoto, N. Umezawa, N. Kato, T. Higuchi, *Chem.—Eur. J.* **2008**, *14*, 8004. d) C. T. Hauser, R. Y. Tsien, *Proc. Natl. Acad. Sci. U.S.A.* **2007**, *104*, 3693. e) S. Lata, M. Gavutis, R. Tampé, J. Piehler, *J. Am. Chem. Soc.* **2006**, *128*, 2365. f) E. G. Guignet, R. Hovius, H. Vogel, *Nat. Biotechnol.* **2004**, *22*, 440.

2 a) A. Rutkowska, C. H. Haering, C. Schultz, *Angew. Chem., Int. Ed.* **2011**, *50*, 12655. b) O. Tour, S. R. Adams, R. A. Kerr, R. M. Meijer, T. J. Sejnowski, R. W. Tsien, R. Y. Tsien, *Nat. Chem. Biol.* **2007**, *3*, 423. c) B. A. Griffin, S. R. Adams, R. Y. Tsien, *Science* **1998**, *281*, 269.

3 N. C. Shaner, P. A. Steinbach, R. Y. Tsien, *Nat. Methods* **2005**, *2*, 905.

4 a) M. J. Hinner, K. Johnsson, *Curr. Opin. Biotechnol.* **2010**, *21*, 766. b) A. Keppler, S. Gendreizig, T. Gronemeyer, H. Pick, H. Vogel, K. Johnsson, *Nat. Biotechnol.* **2002**, *21*, 86.

5 a) S. Uchinomiya, A. Ojida, I. Hamachi, *Inorg. Chem.* **2014**, *53*, 1816. b) H. Nonaka, S. Fujishima, S. Uchinomiya, A. Ojida, I. Hamachi, *J. Am. Chem. Soc.* **2010**, *132*, 9301. c) A. Ojida, K. Honda, D. Shinmi, S. Kiyonaka, Y. Mori, I. Hamachi, *J. Am. Chem. Soc.* **2006**, *128*, 10452.

6 A. Ojida, S. Fujishima, K. Honda, H. Nonaka, S. Uchinomiya, I. Hamachi, *Chem.—Asian J.* **2010**, *5*, 877.

7 a) M. Rekharsky, Y. Inoue, S. Tobey, A. Metzger, E. Anslyn, *J. Am. Chem. Soc.* **2002**, *124*, 14959. b) S. Kubik, R. Kirchner, D. Nolting, J. Seidel, *J. Am. Chem. Soc.* **2002**, *124*, 12752.

8 a) F. Huang, C. Cheng, G. Feng, *J. Org. Chem.* **2012**, *77*, 11405. b) J. A. Drewry, S. Fletcher, H. Hassan, P. T. Gunning, *Org. Biomol. Chem.* **2009**, *7*, 5074.

9 The pK_a values were calculated by Advance Chemistry Development Software (ACD/pK_a, Ver 11.02).

10 H. Nonaka, S. Tsukiji, A. Ojida, I. Hamachi, *J. Am. Chem. Soc.* **2007**, *129*, 15777.

11 The number of alanine residues inserted between the oligo-aspartate unit and the cysteine were previously optimized, in which the spacer with the six alanine residues gave the fastest covalent labeling with a binuclear zinc complex (see Ref. 10).

12 The binding affinity (K_a) of **3**-2Zn(II) with PPi was evaluated to be $2.57 \times 10^6\,M^{-1}$ by ITC experiment (50 mM HEPES, 100 mM NaCl, pH 7.2). This value was larger than that of **1**-2Zn(II) ($K_a = 1.47 \times 10^6\,M^{-1}$) with PPi under the same conditions.

13 The labeling yield of CA6DDAADD-MBP with **7**-2Zn(II) was roughly estimated to be 33% after 10 min based on CBB analysis, in which the relative band intensities of the labeled and unlabeled MBPs were measured. This labeling yield is higher than that of CA6D4-MBP with **8**-2Zn(II) (22% after 10 min), the trend of which agrees with the result of the fluorescence analysis.

14 A. Johansson, M. Abrahamsson, A. Magnuson, P. Huang, J. Mårtensson, S. Styring, L. Hammarström, L. Sun, B. Åkermark, *Inorg. Chem.* **2003**, *42*, 7502.

